PROCEEDINGS OF SCIENCE

Gamma-ray strength functions in the $f_{7/2}$ shell nuclei ^{44,45}Sc and ^{50,51}V

A.C. Larsen[*a†], **M. Guttormsen**[a], **R. Chankova**[b], **F. Ingebretsen**[a], **T. Lönnroth**[c], **S. Messelt**[a], **J. Rekstad**[a], **A. Schiller**[d], **S. Siem**[a], **N.U.H. Syed**[a], **and A. Voinov**[e]

[a] *Department of Physics, University of Oslo*
P.O.Box 1048 Blindern, N-0316 Oslo, Norway
[b] *North Carolina State University, Raleigh, NC 27695, USA*
and Triangle Universities Nuclear Laboratory, Durham, NC 27708 USA
[c] *Department of Physics, Åbo Akademi University*
FIN-20500 Åbo, Finland
[d] *National Superconducting Cyclotron Laboratory, Michigan State University*
East Lansing, MI 48824, USA
[e] *Department of Physics and Astronomy, Ohio University*
Athens, Ohio 45701, USA
E-mail: a.c.larsen@fys.uio.no

The ^{44,45}Sc and ^{50,51}V nuclei have been studied with the pick-up reaction (^{3}He,$\alpha\gamma$) and the inelastic scattering (^{3}He,^{3}He$'\gamma$) for the odd-odd and odd-even isotopes, respectively. From the particle-γ coincidence data, the so-called Oslo method has been applied to extract level density and γ-ray (photon) strength function from primary γ-ray spectra.

In general, the photon strength functions are found to be increasing functions with γ energy. However, for low γ energies ($E_\gamma \leq 3$ MeV), an unexpected enhancement of the photon strength is seen in all the isotopes studied here. As of today, the physical origin of this very interesting feature is not yet revealed.

PACS: 21.10.Ma, 24.10.Pa, 25.55.Hp, 27.70.+q

Workshop on Photon Strength Functions and Related Topics
June 17-20 2007
Prague, Czech Republic

*Speaker.
†This work was supported by the Research Council of Norway (NFR).

PoS(PSF07)008

1. Introduction

The probability of γ decay in an atomic nucleus is governed by the number and character of available final states and the nuclear photon strength function. At low excitation energy, where the density of quantum levels is low, specific transition rates between the levels can be found experimentally. However, for high excitation energy, the level density increases rapidly, and the γ-decay probability is best described by average quantities such as the photon strength function.

The nuclear physics group at the Oslo Cyclotron Laboratory (OCL) has developed a method (the Oslo method) to extract level density and photon strength function simultaneously from particle-γ coincidence data. This work reports on two experiments performed at the OCL on the $f_{7/2}$ shell nuclei $^{44,45}_{21}$Sc [1] and $^{50,51}_{23}$V [2]. These nuclei are of special interest for two reasons. First, they are all relatively light nuclei where the onset of the statistical properties is believed to happen at higher excitation energies than for heavier nuclei. While the scandium isotopes are near mid-shell on the neutron side, they have only one proton outside the $Z = 20$ shell. For the vanadium isotopes the situation is opposite; here, the protons are close to mid-shell when the neutrons (almost) fill the $N = 28$ shell for (^{50}V) ^{51}V. Second, there has been a question whether the previously observed enhancement of the low-E_γ photon strength in ^{56,57}Fe [3] and $^{93-98}$Mo [4] also would appear for the scandium and vanadium isotopes. If this enhancement is found in many nuclei, it might imply that this structure in the strength function is a general feature for a certain mass region. If this is found to be true, it could help to pin down the underlying physics creating this structure.

2. The Oslo Method

The experiments were carried out on natural Sc and V targets with $\sim 99\%$ of ^{45}Sc and ^{51}V. A beam of ^{3}He ions was delivered from the MC-35 Scanditronix cyclotron with energies 38 and 30 MeV on the Sc and V targets, respectively. The pick-up reaction (^{3}He,$\alpha\gamma$) was utilised to study the odd-odd ^{44}Sc and ^{50}V, while the inelastic scattering (^{3}He,^{3}He$'\gamma$) provided data on the odd-even ^{45}Sc and ^{51}V.

The particles and γ rays from the reactions were measured with the multi-detector array CACTUS [5]. From the reaction kinematics, the residual nucleus' excitation energy were calculated from the ejectile energy. The coincidence events were sorted into matrices, for which each excitation-energy bin of 240 keV has its corresponding total γ spectrum. After unfolding the γ-ray spectra [6], the first γ rays emitted in each cascade (first-generation γ rays) were found through a subtraction procedure as described in [7].

The distribution of the first-generation γ rays reveals information on the level density and the γ-ray transmission coefficient. For statistical γ decay in the continuum region, the γ-decay probability from an initial excitation energy E to a final energy $E_f = E - E_\gamma$ is proportional to the γ-ray transmission coefficient $\mathscr{T}(E_\gamma)$ and the level density at the final excitation energy $\rho(E_f)$ [8]:

$$P(E, E_\gamma) \propto \rho(E - E_\gamma)\mathscr{T}(E_\gamma). \tag{2.1}$$

The essential assumption underlying the above relation is that the reaction can be described as a two-stage process, where a compound state is first formed, before it decays in a manner that is independent of the mode of formation [9, 10].The γ-ray transmission coefficient $\mathscr{T}$ is independent of excitation energy according to the generalized Brink-Axel hypothesis [11, 12], which states that collective excitation modes built on excited states have the same properties as those built on the ground state.

Through an iterative procedure [8], the functional form of the level density and the γ-ray transmission coefficient can be determined. However, the slope and the absolute value of both quantities cannot be found from the iteration process. Therefore, data from other sources are applied for this purpose.

3. Level densities

The experimental level densities are normalized to known, discrete levels at low excitation energy. From neutron (or proton) resonance experiments, the energy spacing between the levels reached by this reaction is used to calculate the total level density at the neutron (or proton) binding energy (see Ref. [8]). The level density functions are then adjusted so that they agree with both the low-energy data and the level density at B_n (B_p). For more details, see [1, 2, 8].

The obtained level densities for ^{44,45}Sc and ^{50,51}V are shown in Fig. 1. In general, roughly speaking, they all increase exponentially as a function of excitation energy. The level density of ^{51}V differs from the others in the respect that it shows large bumps and structures up to ~ 5 MeV of excitation energy. These features are interpreted as effects of the $N = 28$ shell gap, which also lowers the number of available levels in this nucleus considerably at low excitation energy compared to ^{50}V.

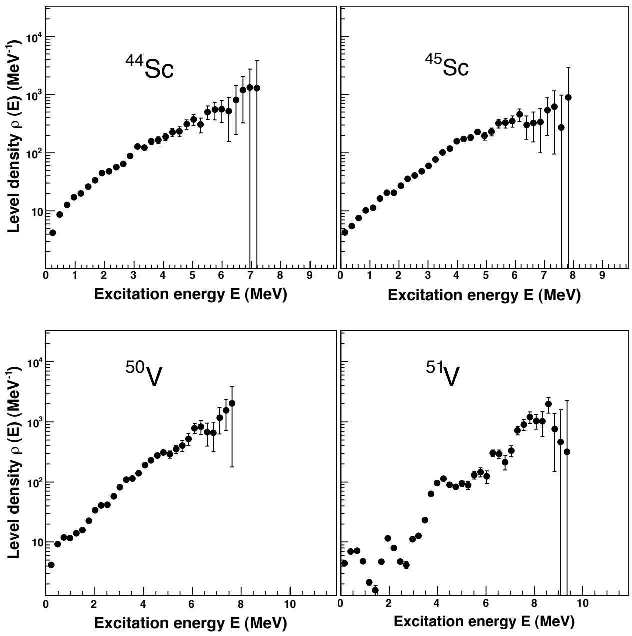

Figure 1: Level densities of ^{44,45}Sc and ^{50,51}V.

4. Photon strength functions

By using the Oslo method, also the total γ-ray transmission coefficient can be extracted from the experimental data. The total γ-ray transmission coefficient $\mathscr{T}(E_\gamma)$ is directly proportional to the total photon strength function $f(E_\gamma)$ as seen by the relation

$$\mathscr{T}(E_\gamma) = \sum_{XL} \mathscr{T}_{XL} = 2\pi \sum_{XL} E_\gamma^{2L+1} f_{XL}(E_\gamma), \tag{4.1}$$

where $\mathscr{T}_{XL}$ and f_{XL} is the γ-ray transmission coefficient and photon strength function, respectively, for electromagnetic character X and multipolarity L. By assuming that dipole radiation ($L = 1$) is dominant, the experimental γ-ray transmission coefficient can be converted into photon strength by

$$f(E_\gamma) \simeq \frac{1}{2\pi} \frac{\mathscr{T}(E_\gamma)}{E_\gamma^3}. \tag{4.2}$$

The slope of the γ-ray transmission coefficient $\mathscr{T}(E_\gamma)$ has already been determined through the normalization of the level densities. Data on the average total radiative width $\langle\Gamma_\gamma\rangle$ at B_n or experimental data on f_{E1} and f_{M1} provide the absolute value of $\mathscr{T}$ [1, 2]. The normalized photon strength functions of ^{44,45}Sc and ^{50,51}V are displayed in Fig. 2.

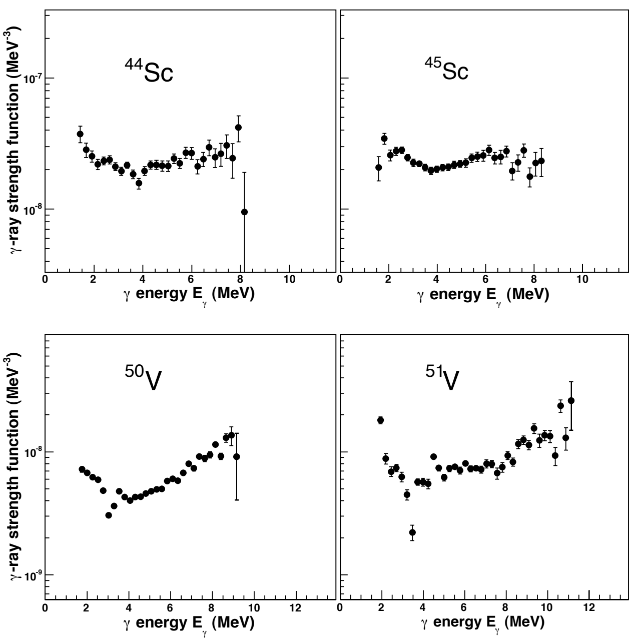

Figure 2: Photon strength functions of ^{44,45}Sc and ^{50,51}V.

Several interesting features of the photon strength functions can be seen in Fig. 2. In general, for $E_\gamma \geq 3.5$ MeV, the data show that all the photon strength functions are increasing with γ energy. For γ energies below ~ 3 MeV, the photon strength functions have an increase of a factor of $\sim 2-3$ relative to their minimum.

To investigate the experimental strength functions further, they are compared to theoretical predictions. Here this comparison is demonstrated for the ^{44}Sc case. The $E1$ part of the total γ-strength function has been described by the Kadmenskiĭ, Markushev and Furman (KMF) model [13] by

$$f_{E1}(E_\gamma) = \frac{1}{3\pi^2\hbar^2c^2}\frac{0.7\sigma_{E1}\Gamma_{E1}^2(E_\gamma^2+4\pi^2T^2)}{E_{E1}(E_\gamma^2-E_{E1}^2)^2}. \tag{4.3}$$

Here, σ_{E1} is the cross section, Γ_{E1} is the width, and E_{E1} is the centroid of the giant electric dipole resonance (GEDR). The Lorentzian parameters are taken from [14]. The nuclear temperature of the final state, introduced to ensure a nonvanishing GEDR for $E_\gamma \to 0$, is given by $T(E_f) = \sqrt{U_f/a}$.

For the magnetic dipole strength f_{M1}, the Lorentzian giant magnetic dipole resonance (GMDR) (the spin-flip $M1$ resonance) is applied [15]:

$$f_{M1}(E_\gamma) = \frac{1}{3\pi^2\hbar^2c^2}\frac{\sigma_{M1}E_\gamma\Gamma_{M1}^2}{(E_\gamma^2-E_{M1}^2)^2+E_\gamma^2\Gamma_{M1}^2}. \tag{4.4}$$

The contribution from $E2$ radiation to the total strength function is assumed to be very small. However, for the sake of completeness, the $E2$ isoscalar reconance described by

$$f_{E2}(E_\gamma) = \frac{1}{5\pi^2\hbar^2c^2E_\gamma^2}\frac{\sigma_{E2}E_\gamma\Gamma_{E2}^2}{(E_\gamma^2-E_{E2}^2)^2+E_\gamma^2\Gamma_{E2}^2} \tag{4.5}$$

is included in the total, theoretical strength function.

In lack of any established theoretical prediction of the observed increase at low γ energy, this phenomenon is modelled by a simple power law as

$$f_{\text{upbend}}(E_\gamma) = \frac{1}{3\pi^2\hbar^2c^2}AE_\gamma^{-b}, \tag{4.6}$$

where A and b are fit parameters.

The total, theoretical γ-ray strength function is then given by

$$f_{\text{total}} = \kappa(f_{E1}+f_{M1}+f_{\text{upbend}})+E_\gamma^2 f_{E2}, \tag{4.7}$$

where κ is a renormalization factor that should be close to unity. The result for ^{44}Sc is displayed in Fig. 3. It is seen that the theoretical strength function fits the data well. From Fig. 3, one would also conclude that the data points below ~ 3 MeV are not described by the standard models.

In Fig. 3 also the sum of the photoneutron cross-section data from the reaction ^{45}Sc(γ,n) [16] and the photoproton cross-section data from the reaction ^{45}Sc(γ,p) [17] are shown. The photoabsorbtion cross-section $\sigma(E_\gamma)$ is converted into strength function through the relation

$$f(E_\gamma) = \frac{1}{3\pi^2\hbar^2c^2}\cdot\frac{\sigma(E_\gamma)}{E_\gamma}. \tag{4.8}$$

The (γ,n) and (γ,p) data seem to fit reasonably well with the theoretical expectation and the Oslo data. Note that the photoabsorbtion cross-sections from the (γ,n) and (γ,p) reactions may have some overlap in strength in the energy region where the (γ,pn) channel is opened.

The enhancement of the photon strength functions at low γ energies previously seen in ^{56,57}Fe [3] and $^{93-98}$Mo [4], has now been established also in the Sc and V isotopes studied here. As has been shown in Fig. 3, none of the standard models can account for this behaviour. It is evident that the increased strength at low γ energies should be confirmed by independent experiments such as the two-step cascade technique also for these nuclei. Also, it is mandatory to determine the electromagnetic character and the multipolarity of the structure to be able to suggest its physical origin.

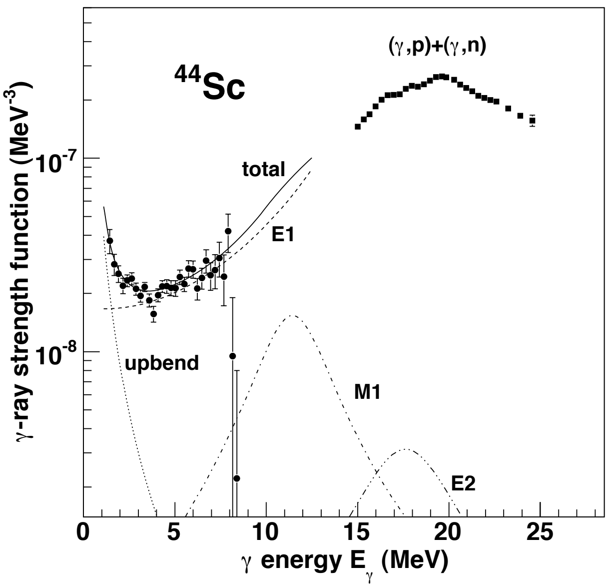

Figure 3: Photon strength function of ^{44}Sc from Oslo data (black points) compared with theoretical $E1$ strength (dashed line), $M1$ spin-flip resonance (dashed-dotted line) and isoscalar $E2$ resonance (dashed-dotted line). A fit to the upbend structure (dotted line) and the total, theoretical photon strength function (solid line) are also shown. Summed photo-absorbtion cross section data from ^{45}Sc(γ,p) and ^{45}Sc(γ,n) are displayed as black squares.

5. Summary

The experimental level densities and photon strength functions of ^{44,45}Sc and ^{50,51}V extracted from primary γ spectra with the Oslo method have been presented. The photon strength functions of all nuclei shown here display an increase with increasing γ energy for $E_\gamma \geq 3$ MeV, but also a big enhancement of strength at low γ energies. This fascinating behaviour has at present no unequivocal explanation.

References

[1] A.C. Larsen, M. Guttormsen, R. Chankova, T. Lönnroth, S. Messelt, F. Ingebretsen, J. Rekstad, A. Schiller, S. Siem, N.U.H. Syed, and A. Voinov, http://arxiv.org/abs/0706.0533v1, submitted to Phys. Rev. C.

[2] A.C. Larsen, R. Chankova, M. Guttormsen, F. Ingebretsen, T. Lönnroth, S. Messelt, J. Rekstad, A. Schiller, S. Siem, N.U.H. Syed, A. Voinov, and S.W. Ødegård, Phys. Rev. C **73**, 064301 (2006).

[3] A. Voinov, E. Algin, U. Agvaanluvsan, T. Belgya, R. Chankova, M. Guttormsen, G.E. Mitchell, J. Rekstad, A. Schiller and S. Siem, Phys. Rev. Lett **93**, 142504 (2004).

[4] M. Guttormsen, R. Chankova, U. Agvaanluvsan, E. Algin, L.A. Bernstein, F. Ingebretsen, T. Lönnroth, S. Messelt, G.E. Mitchell, J. Rekstad, A. Schiller, S. Siem, A.C. Sunde, A. Voinov and S. Ødegård, Phys. Rev. C **71**, 044307 (2005).

[5] M. Guttormsen, A. Atac, G. Løvhøiden, S. Messelt, T. Ramsøy, J. Rekstad, T.F. Thorsteinsen, T.S. Tveter, and Z. Zelazny, Phys. Scr. **T 32**, 54 (1990).

[6] M. Guttormsen, T.S. Tveter, L. Bergholt, F. Ingebretsen, and J. Rekstad, Nucl. Instrum. Methods Phys. Res. A **374**, 371 (1996).

[7] M. Guttormsen, T. Ramsøy, and J. Rekstad, Nucl. Instrum. Methods Phys. Res. A **255**, 518 (1987).

[8] A. Schiller, L. Bergholt, M. Guttormsen, E. Melby, J. Rekstad, and S. Siem, Nucl. Instrum. Methods Phys. Res. A **447**, 498 (2000).

[9] A. Bohr and B. Mottelson, *Nuclear Structure*, (Benjamin, New York, 1969), Vol. I, p. 169, p. 184-185.

[10] L. Henden, L. Bergholt, M. Guttormsen, J. Rekstad, and T.S. Tveter, Nucl. Phys. **A589**, 249 (1995).

[11] D. M. Brink, Ph.D. thesis, Oxford University, 1955.

[12] P. Axel, Phys. Rev. **126**, 671 (1962).

[13] S.G. Kadmenskiĭ, V.P. Markushev, and V.I. Furman, Yad. Fiz. **37**, 277 (1983) [Sov. J. Nucl. Phys. **37**, 165 (1983)].

[14] Centre for Photonuclear Experiments Data, http://cdfe.sinp.msu.ru

[15] A. Voinov, M. Guttormsen, E. Melby, J. Rekstad, A. Schiller, and S. Siem, Phys. Rev. C **63**, 044313 (2001).

[16] A. Veyssiere, H. Beil, R. Bergere, P. Carlos, A. Lepretre, and A. de Miniac, Nucl. Phys. **A227**, 513 (1974).

[17] S. Oikawa and K. Shoda, Nucl. Phys. **A277**, 301 (1977).